

Online ISSN: 2682-2628

Print ISSN: 2682-261X

# IJC CBR

## INTERNATIONAL JOURNAL OF CANCER AND BIOMEDICAL RESEARCH

<https://jcbr.journals.ekb.eg>

Editor-in-chief

Prof. Mohamed Labib Salem, PhD

**The diagnostic efficacy of tailored  
multiparametric breast MRI in indeterminate  
mammographic lesions: a single tertiary  
oncology center**

Gehan S. Seifeldin, Tarek M. Elsaba, Adel Gabr, Dalia O.  
Mohamed, Summer Elmorshidy, Haisam Atta



PUBLISHED BY

**EACR** EGYPTIAN ASSOCIATION  
FOR CANCER RESEARCH

Since 2014

**International Journal of Cancer & Biomedical Research  
(IJCBR) <https://jcbr.journals.ekb.eg>**

IJCBR is an Int. journal published by the Egyptian Society of Cancer Research (EACR, established in 2014, <http://eacr.tanta.edu.eg>) and sponsored by the Egyptian Knowledge Bank (EKB: [www.ekb.eg](http://www.ekb.eg)).

IJCBR has been approved by the Supreme Council of Universities, Egypt with score 7 (<http://egjournal.scu.eg>). The journal is cited by google scholar and registered by Publons (<https://publons.com>). The journal has recently been evaluated in 2020 by Nature Springer with a good standing.

**Scope of IJCBR**

- Drug discovery from natural and synthetic resources
- BioMedical applications of nanotechnology
- Sem cell biology and its application
- Basic and applied biotechnology
- Inflammation and autoimmune diseases
- In silico models and bioinformatics
- In vitro and In vivo preclinical animal models
- Cellular and molecular cancer biology
- Cancer Immunology and Immunotherapy
- New methods for prediction, early detection, diagnosis prognosis and treatment of diseases.
- Immunology in health and diseases
- Anti-microbial defense mechanisms
- Cellular and molecular physiology and pathology of diseases

**IJCBR Editor,**  
**Prof. Mohamed Labib Salem, PhD**  
Professor of Immunology  
Faculty of Science, Tanta University, Egypt

## The diagnostic efficacy of tailored multiparametric breast MRI in indeterminate mammographic lesions: a single tertiary oncology center

Gehan S. Seifeldein<sup>1</sup>, Tarek M. Elsaba<sup>2</sup>, Adel Gabr<sup>3</sup>, Dalia O. Mohamed<sup>4</sup>, Summer Elmorshidy<sup>5</sup>, Haisam Atta<sup>6</sup>

<sup>1</sup> Diagnostic and interventional radiology Department, Assiut University, Egypt.

<sup>2</sup> Pathology Department, South Egypt Cancer Institute, Assiut University, Egypt

<sup>3</sup> Medical Oncology Department, South Egypt Cancer Institute, Assiut University, Egypt

<sup>4</sup> Radiotherapy Department, South Egypt Cancer Institute, Assiut University, Egypt

<sup>5</sup> Clinical Oncology Department, Faculty of Medicine, Assiut University, Egypt

<sup>6</sup> Radiology Department, South Egypt Cancer Institute, Assiut University, Egypt

### ABSTRACT

**Objectives:** Assessing the diagnostic role of multiparametric MRI (mpMRI) in indeterminate mammographic breast lesions and postulated a diagnostic model for MRI interpretation integrating the morphological and functional parameters. **Material and Methods:** Two hundred forty patients included in a self-control retrospective study in a tertiary center. All patients examined with 1.5T MR unit using multiparametric studies, including morphological analysis followed by functional evaluation via MR diffusion (MR-DWI), spectroscopy (MRS), and kinetic enhanced curves (DCE-MRI). Diagnostic performance of each parameter evaluated alone and in combination. The histopathological results were the standard of reference. **Results:** Combined mpMRI parameters possess a moderate agreement ( $\kappa=0.435$ ) with a 23.5% false discovery rate (FDR) and an overall accuracy of 78%. On the other hand, combined mpMRI data after omitting MRS data show almost perfect agreement ( $\kappa=0.923$ ) with histopathological data and recorded 100% specificity, 90% specificity, 5% FDR and zero% for both false omission rate (FOR) and false-negative rate (FNR). The Quantitative analysis of DWI with ADC map shows a significant statistical value for mean ADC (m-ADC) value and relative ADC (r-ADC) value. The former has cutoff value  $1.1 \times 10^{-3} \text{ mm}^2/\text{sec}$  with higher specificity 97.5% while r-ADC has cutoff value  $0.42 \times 10^{-3} \text{ mm}^2/\text{sec}$  with quite lower specificity 85%. Perfect agreement in the interpretation of DCE-MRI curves, MR-DWI, and MRS with  $\kappa=0.92, 0.9$  and  $0.84$ , respectively. **Conclusion:** Tailored combined multiparametric MRI is a potent diagnostic tool in the characterization of indeterminate mammographic breast lesions.

**Keywords:** MRI, multiparametric, diffusion-weighted imaging, magnetic resonance spectroscopy, BI-RADS

Editor-in-Chief: Prof. M.L. Salem, PhD - Article DOI: 10.21608/IJCBR.2020.36193.1057

### ARTICLE INFO



#### Article history

Received: July 18, 2020

Revised: August 30, 2020

Accepted: September 21, 2020

#### Correspondence to:

Haisam Atta, MD  
Department of Radiology,  
South Egypt Cancer Institute,  
Assiut University, Egypt  
Mobile: (+20) 1005017866  
Email: haisamasa@aun.edu.eg

## INTRODUCTION

Conventional mammography and ultrasound are the first traditional steps for evaluation of suspicious breast lumps. The lesions' morphology in terms of speculations with ill-defined margins or presence of comedo calcifications, lead to the development of Breast Imaging Reporting and Data System (BI-RADS). BI-RADS 3,4 categories are labeled indeterminate with a different burden of neoplastic lesions. The inconclusive nature of

such lesions results in a large number of unavoidable biopsies (Pinker et al., 2011; Fowler, 2014). Breast MRI is a valuable complementary tool in the evaluation of neoplastic lesions; however, there is still no clear consensus on its employment in inconclusive sono-mammographic findings (El Khoury et al., 2015; Shimauchi et al., 2018). Moreover, advances in breast MRI techniques led to an improvement in the specificity of such methods, including multiple pre- and post-contrast sequences with and without fat

suppression and functional imaging studies (Mango et al., 2015; Shimauchi et al., 2018).

Functional MR imaging modalities show metabolic alterations in breast tissue that may be useful in the further evaluation of suspicious breast lumps by magnetic resonance spectroscopy (MRS). In contrast, MR diffusion-weighted imaging (DWI) provides some insight into lesion cellularity. Moreover, the vascularity data is provided by dynamic contrast enhancement (DCE), reflecting the presence of neoangiogenesis (Pinker et al., 2011; Fowler, 2014). On DCE-MRI, the resultant kinetic curve is very suggestive of breast cancer even though the enhancement pattern has been found in a small proportion of breast cancer patients. Bluemke et al. (2004) reported low sensitivity and high specificity for the washout of enhancement as an indicator of malignancy. Moreover, Schnall et al. (2006) stated that reliance on a kinetic curve assessment alone is not sufficient as there is an overlap between benign and malignant lesions regarding the enhancement patterns. DWI is an essential tool in breast lesions characterization. Even in its quantitative assessment, breast cancer has lower mean ADC values compared to benign lesions and normal breast tissue (Razek et al., 2010). Moreover, the choline peak at MRS can be used as a marker of malignancy (Baek, 2012). The employment of functional and morphological data delivered the concept of multiparametric MRI (Mp-MRI) as a recent approach for characterization of breast lesions (Pinker et al., 2011). However, there is still a discrepancy between reported accuracy and feasibility of the multiparametric data (Aribal et al., 2016). Few studies handled the integration of MRI in the characterization of BI-RADS 3 and 4 lesions. Akita et al. (2009) confined their evaluation to morphological parameters, while other authors handled DCE-MRI (Gökalp and Topal, 2006; Cilotti et al., 2007; Uematsu et al., 2007; Moy et al., 2009). Many authors investigate these functional MRI parameters solely and in combination. This combination was created to overcome the limitations in specificity when dealing with these parameters separately and to improve their diagnostic performance (Pinker et al., 2017).

The current study is aiming to assess the diagnostic role of mpMRI in indeterminate mammographic breast lesions (BI-RADS 3 and 4) and to postulate a diagnostic model for MRI interpretation integrating the different parameters in characterization of these lesions.

## MATERIAL AND METHODS

### Study Design and Inclusion criteria

A retrospective self-control study, including 240 patients: with histopathological confirmation, of 160 malignant cases, in a tertiary oncology center. The local ethics board approved the study. Written informed consent was waived concerning the nature of the study. In The retrospective search, all patients were identified via a prospectively maintained database, revealed 321 female patients with BI-RADS 3 and 4 lesions in the period from January 2016 to December 2018. The population was acquired from a non-screening community-based on a suspicious clinical examination or subjects with a strongly positive family history either in their first or second-degree relatives, or even subjects with other different established risk factors (McPherson, 2000).

Cases were included in the study if their database included mpMRI, including the morphological and functional data (DWI, DCE, and MRS); and histopathological results. The correlation was performed either with ultrasound-guided biopsy or surgical biopsy. We excluded 81 cases; Forty-one cases were excluded as they were managed conservatively without biopsy or were missed (did not show up for further management in our center). Further, 40 cases were excluded as their MR studies were missing part of functional MR data: MR DWI sequence (5 cases) or MRS sequence (35 cases) (Figure 1). Two hundred eight patients were estimated to be the minimum sample size required to carry out the study according to the sample size equation for descriptive research (Leonard and Arnold, 1961). The validity measures were 60%, with an error probability of 0.05 and 95% power. The sample was raised to include 240 as follows:

$$N = (z_{1-\alpha/2})^2 P(1-P) / D^2$$

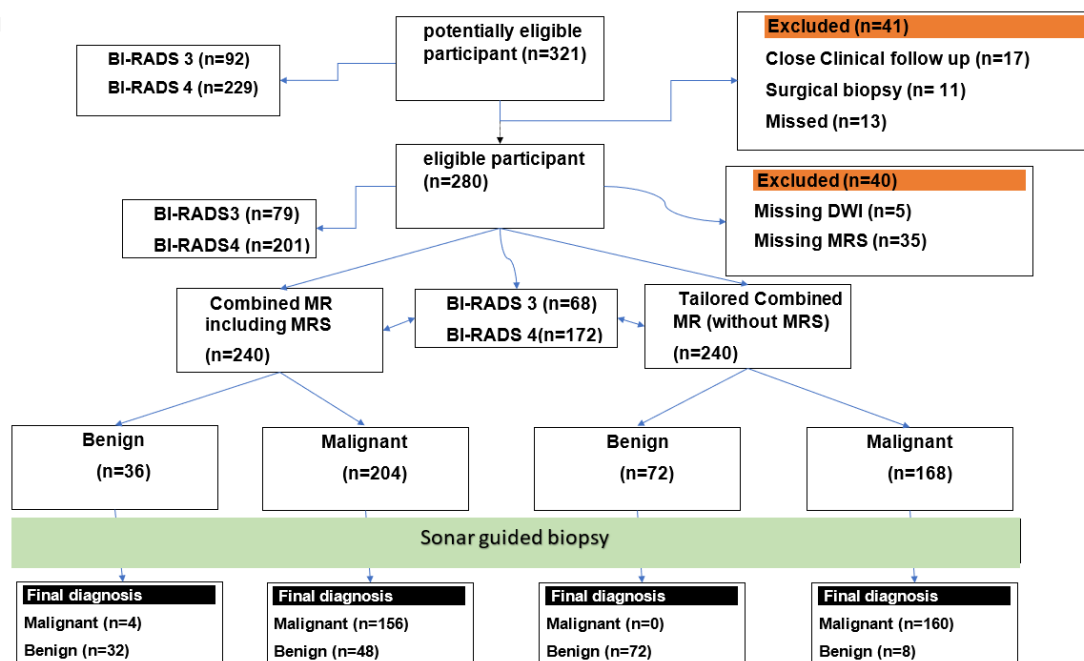


Figure 1. STARD diagram to report case flow within the study.

Table 1. Technical parameters of the employed MR sequences

Parameter of sequences	T2-WI axial (TSE)	T2-WI fat-suppressed axial	T1-WI without fat-suppression Axial	DWI* Axial	3D T1 GRE Axial with fat saturation	MRS -single voxel (PRESS)**
TR (ms)	5300	5250	1420	5900	113	1500
TE (ms)	60	58	12	93	5	100
Flip angle (FA)	180°	142°	180°		20°	90°
Slice thickness (mm)	5.5	5	6	5	1.2	
Field of view (FOV) (mm)	340	360	450	400	360	
Matrix (pixels)	512x384	512x256	256x160	192x192	384x384	
Spacing	No space	20%	5%	30%	No space	
Voxel size in mm	1.2x0.9x5.5	1.3x1.1x5.0	2.1x1.4x6.0	2.2x2.1x5.8	1.6x1.1x1.2	15x15x15
Acquisition time (minutes)	2.51	2.39	2.14	2.04	4.18	3.18

\*b values of 50,400, 800 sec/mm<sup>2</sup>, fat saturation by water excitation, \*\*Fat and water suppression using conventional CHESS pulses

### Mammography and interpretation

A breast mammographic examination was performed with Senographe-DMR, GE. The classic employed views are craniocaudal and mediolateral views with compression. The breast tissue density in mammography was scored as categories A through D. The interpretation of the studies was conducted according to BI-RADS lexicon fifth edition (Rao et al., 2016).

### Breast MRI Technique

Scans were performed on MRI Machine is 1.5 T (Magnetom Avanto, Siemens Healthcare) using a dedicated eight-channel breast coil where the patient is positioned in a prone position to fit and adjust both breasts within the coil. Pre-contrast sequences include axial T2WI with fat

suppression and Axial DWI. The employed b factors were b 50, 400, and 800 sec/mm<sup>2</sup>. An apparent diffusion coefficient (ADC) map was created with the involvement of all of the b values. The post-contrast sequences were initiated by DCE, which is acquired by a 3D fat suppression sequences with a pre-injection 3D T1WI and followed by five multiplanar post-contrast T1WI measures, each last for 1 minute. The subtracted images were considered as a reference. The contrast-enhanced kinetic curve was postulated among the classic types, according to Kuhl et al. (2007) The used contrast material is Gadolinium pentate (Magnevist™), with a dose of injection of 0.1 mmol/kg via an automatic injector with a 2 ml/sec rate followed by a 20 ml isotonic saline flush administered using an automatic injector. Single voxel proton

(<sup>1</sup>H)-MRS; using point resolved spectroscopy (PRESS); is performed and the image acquisition by a single voxel with TE 100 ms. The voxel was centered on the enhanced component of the lesion. The technical parameters of the employed MR sequences are summarized in Table 1.

### MRI interpretation

MR studies were evaluated by two senior radiologists (18-20 years' experience) who interpreted the MR images separately blinded to the other reports or the histopathological results. Cases were enrolled in the study by oncologists after revising their clinical data. The morphological analysis was based on native T1WI and T2WI with/without fat suppression sequence and DCE-MRI. Firstly, regarding T1 and T2 signal the lesion interpreted as follow: according to Stusinska et al. (2014) lesions with high signal on both T2 WI and T2WI with fat suppression and low signal on T1WI interpreted as a benign lesion with high water content like a cyst with exception mucinous carcinoma, while those of high signal on both T1WI and T2WI and low signal on T2WI fat suppression interpreted as benign lesion containing fat component. On the other hand, those lesion of low or intermediate signal on T1WI, T2WI, and intermediate or high on T2WI with fat suppression were interpreted as a suspicious lesion of malignancy. While those show low signal on T1WI and very low signal on T2WI and intermediate on T2WI with fat suppression were interpreted as fibrotic lesions (Stusińska et al., 2014).

Regrading DCE, the subtracted images used to assess the presence of enhancing mass or non-mass enhancement lesions, where the enhancing mass lesions evaluation was based on the American College of Radiology (ACR) BI-RADS fifth edition (Rao et al., 2016). While the enhancing non-mass lesions were evaluated according to the three-step interpretation, according to Schimauchi et al. (2016) Secondly, by evaluating the semiquantitative kinetic enhancement characteristics curves was quantified by placed ROI placed in the areas of the strongest abnormal enhancement and size of the ROI adjusted to the size of the enhancing lesion. However, it should be greater than three

pixels (Kuhl et al., 1999; Spak et al., 2017). The type of the delayed-enhancement patterns of the DCE curve is recorded according to Kuhl et al. (1999) as follows: Type I is a steady persistent, the signal intensity continues to increase over the entire time. Type II is a plateau in which there is an initial upstroke, and the signal intensity plateaus in the intermediate and late postcontrast periods. Type III is a washout in which there is an initial upstroke, after which enhancement is abruptly decreased (washes out) in the intermediate postcontrast period (i.e., 2–3minutes after injection of contrast material). Type II and III favor malignant nature.

MRI-DWI analysis includes both qualitative and quantitative assessments. The qualitative assessment detects if there is restricted or facilitated MR diffusion as restriction indicates hypercellularity and favors neoplastic nature (Greenwood et al., 2018). The quantitative evaluation of MRI-DWI is done by integrating different parameters, including minimum ADC (min-ADC), maximum ADC, mean ADC (m-ADC), and the difference ADC (d-ADC) that is calculated by subtracting the min-ADC from the maximum ADC. This quantitative data is calculated by applying a circular region of interest (ROI) on the lowest signal portion of the lesion. Another ROI is applied to the contralateral breast fibro-glandular tissue, which is considered as a reference organ, according to Park et al. (2007) and hence the self-control portion of the study. (Figure 2). The relative ADC (r-ADC) is calculated by dividing m-ADC of the lesion by that of the contralateral breast, according to Yilmaz et al. (2018).

The MRS interpretation is based on the total choline-containing compounds (tCho) resonance in qualitatively determined breast spectra. tCho peak position should be recorded in the metabolite spectrum. According to Haddadin et al. (2009|), *In vivo* breast, MR spectra detect tCho at resonance at 3.2 ppm that was the criterion for determining the presence or absence of Cho, and it is known to be associated with malignancy (Bartella and Huang, 2007).

### Combined Mp-MRI parameter interpretation

The MR data, including morphology, DCE-MRI, DWI, and MRS, was utilized to create combined

parameter for differentiation as when two or more of the parameters mentioned above are positive, the combined parameter impression is considered positive for the presence of malignancy (Aribal et al., 2016).

**Histopathological correlation**

The pathologist was blind to the results of imaging at the time of evaluation. Microscopic examination was performed after preparation and staining with Hematoxylin and eosin stain (H and E) to document the malignant or benign nature of the lesions (Figure 3).

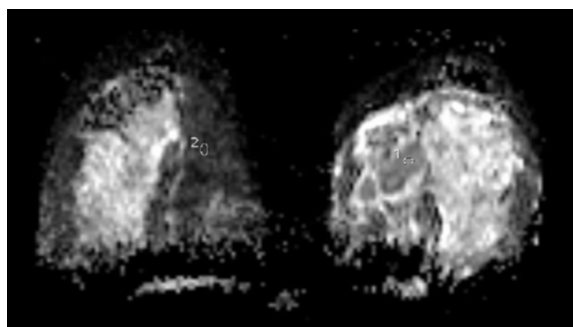


**Figure 2.** Demonstration of applying the ROI on the right breast lesion to calculate the minimum, maximum, difference and mean ADC, second ROI applied on contralateral breast parenchyma to calculate the relative ADC.

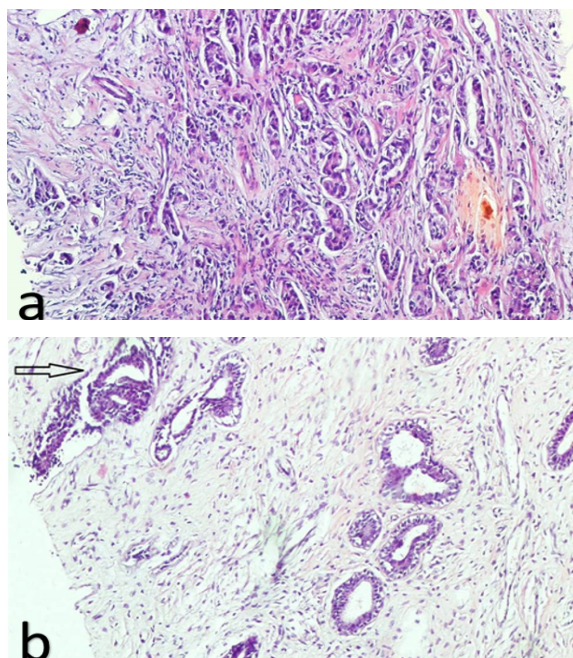


**Figure 3.** Microscopic image from a True cut needle biopsy of breast lesions (A) represents a case of invasive ductal carcinoma showing malignant cells within a desmoplastic stroma (B) represents a case of fibrocystic disease of the breast showing fibrous tissue with entrapped ducts with a focus of ductal epithelial hyperplasia (arrow).

**Statistical analysis**

Categorical data were described using mean and standard deviations, while ordinal data were expressed using frequencies. The weighted Cohen's Kappa was employed to assess the agreement between pathological results, the MRI diagnostic parameters, in addition to the interrater reliability. Validity statistics including sensitivity, specificity, positive and negative predictive value –PPV & NPV-, False Positive Rate, False Negative Rate – FPR & FNR-, False Discovery Rate, False Omission Rate –FDR & FOR-, were calculated. Evaluation of the cutoff value was done using the receiver operating characteristic (ROC) curve for m-ADC and choline position in MRS of benign and malignant lesions and analyzed as the area under the curve (AUC), standard error (SE) and 95% confidence interval (CI). Results were considered statistically significant when the p-value is  $p < 0.05$ . IBM-SPSS version 21 was used for statistical analysis.

**RESULTS**

**Patients' demographic data**

The patients' age ranged from 28 to 70 years, with a mean age of  $47.8 \pm 11.0$  years. Among the malignant cases, 116/160 (72.5%) cases were in post-menopausal status, whereas 56 cases had late menopause. The recorded data showed 59/160 (36.9%) patients with early menarche. Moreover, 44/160 (27.5%) of malignant cases were in pre-menopausal status. The incidence of positive family history was recorded in 28/160 (17.5%) of malignant cases, whereas 41% of them had a positive first-degree relative, while 59% had a second degree relative with a positive history, as mentioned in Table 2.

**Table 2.** Baseline Demographic Characteristics of Study Cohort

Parameter		n = 240
Age in years	Mean $\pm$ SD	47.80 $\pm$ 11.0
	Median (IQR)	46.5 (15)
Menstrual Status	Pre-	108 (45%)
	Post-	132 (55%)
Family History	Negative	208 (86.7%)
	Positive	32 (13.3%)
Mammographic BIRADS	BIRAD 3	68 (28.3%)
	BIRAD 4	172 (71.7%)

### Mode of biopsy and histopathological results

Surgical biopsy was employed in 139 cases; 93 cases among them were proven to be malignant. While sonar guided biopsy was performed in 101 cases, 34 cases of them were proven to be benign. Pathological records showed five varieties of benign diseases, where fibroadenoma has the highest frequency encountered in 32 cases. While the malignant neoplasms records have five types, the most commonly encountered variety was invasive duct carcinoma in 112 patients.

### MRI Results

Different MRI parameters show significant statistical results regarding the variable degree of agreement with histopathological findings (Table 3). MRI-DWI showed almost perfect agreement ( $\kappa=0.93$ ,  $p<0.001$ ) with an

agreement in 96.6% of cases, with high validity measures (Table 4) recording 100% regarding specificity and positive predictive value (PPV) while the false-negative rate (FNR) is 5% and false discovery rate (FDR) is 0%.

In comparison, the false omission rate (FOR) recorded 9%, with an overall accuracy of 97% (Figure 4). The quantitative parameters in the evaluation of the ADC map showed a significant statistical value for m-ADC value and r-ADC value. The former had cutoff value  $1.1 \times 10^{-3}$  mm<sup>2</sup>/sec with higher specificity 97.5% while r-ADC had cutoff value  $0.42 \times 10^{-3}$  mm<sup>2</sup>/sec with quite lower specificity 85% (Figure 5). The lowest rank of the employed quantitative assessment of the ADC map is recorded with a d-ADC cutoff value  $0.06 \times 10^{-3}$  mm<sup>2</sup>/sec with a 50% PPV (Table 5).

Table 3. Agreement between Pathology Results and Different MRI Parameters

	Tumor Pathology			Total
		Benign	Malignant	
Morphology Impression	Benign	68 (28.3%)	4 (1.7%)	72 (30%)
	Malignant	12 (5.0%)	156 (65%)	168 (70%)
Total		80 (33.3%)	160 (66.7%)	240 (100%)
Weighted Kappa Coefficient		0.846		P < 0.001
Chi-square test		172.9		P < 0.001
Curve Impression	Benign	72 (30%)	16 (6.7%)	88 (36.7%)
	Malignant	8 (3.3%)	144 (60%)	152 (63.3%)
Total		80 (33.3%)	160 (66.7%)	240 (100%)
Weighted Kappa Coefficient		0.800		P < 0.001
Chi-square test		216.0		P < 0.001
Spectroscopy Impression	Benign	32 (13.3%)	96 (40.0%)	128 (53.3%)
	Malignant	48 (20.0%)	64 (26.7%)	112 (46.7%)
Total		80 (33.3%)	160 (66.7%)	240 (100%)
Weighted Kappa Coefficient		-0.174		P = 0.003
Chi-square test		8.6		P = 0.003
Diffusion Impression	Benign	80 (33.3%)	8 (3.3%)	88 (36.7%)
	Malignant	0 (0.0%)	152 (63.3%)	152 (63.3%)
Total		80 (33.3%)	160 (66.7%)	240 (100%)
Weighted Kappa Coefficient		0.927		P < 0.001
Chi-square test		207.3		P < 0.001
Combined Impression*	Benign	32 (13.3%)	4 (1.7%)	36 (15%)
	Malignant	48 (20.0%)	156 (65%)	204 (85%)
Total		80 (33.3%)	160 (66.7%)	240 (100%)
Weighted Kappa Coefficient		0.435		P < 0.001
Chi-square test		58.8		P < 0.001
Tailored Combined Impression-	Benign	72 (13.3%)	0 (1.7%)	72 (30%)
	Malignant	8 (20.0%)	160 (65%)	168 (70%)
Total		80 (33.3%)	160 (66.7%)	240 (100%)
Weighted Kappa Coefficient		0.923		P < 0.001
Chi-square test		58.8		P < 0.001

**Table 4.** Validity Measures of the Different MRI Parameters

Measure	Morphology	Curve	Spectroscopy	Diffusion	Combined MR parameter	Tailored Combined MR parameter
Sensitivity	97.5%	90%	40%	95%	97.5%	100%
Specificity	85%	90%	40%	100%	40%	90%
PPV	93%	95%	57%	100%	76.5%	95%
NPV	94.5%	82%	25%	91%	89%	100%
Accuracy	93.3%	90%	40%	97%	78%	97%
FNR	2.5%	10%	60%	5%	2.5%	0%
FPR	15%	10%	60%	0%	60%	10%
FDR	7%	5%	43%	0%	23.5%	5%
FOR	6%	18%	75%	9%	11%	0%

PPV=Positive Predictive Value, NPV=Negative Predictive Value, FPR=False Positive Rate, FNR=False Negative Rate, FDR=False Discovery Rate, FOR=False Omission Rate

**Table 5.** Diagnostic performance of Apparent Diffusion Coefficient (ADC) Parameters for Breast cancer Prediction, analyzed as the area under the curve

	Mean ADC	R. ADC	Min. ADC	Diff. ADC
AUC*	0.992 (<0.001)	0.992 (<0.001)	0.928 (<0.001)	0.287 (<0.001)
CI**	0.854-1.000	0.889-1.000	0.827-0.975	0.097-0.412
SE***	0.021	0.044	0.053	0.077
Cutoff	1.11	0.42	0.82	0.06
Sensitivity	95%	100%	90%	90%
Specificity	97.5%	85%	85%	10%
PPV	97%	87%	86%	50%
NPV	95%	100%	89.5%	50%

\*AUC = Area under the Curve, \*\*CI = Confidence Interval, \*\*\*SE = Standard Error, \*Null hypothesis: true area = 0.5

The morphological analysis showed a strong agreement with pathological results ( $\kappa = 0.846$ ,  $p < 0.001$ ) with an agreement in 90% of cases with 6% FOR, 7% FDR, 93.3% in overall accuracy, and 85% specificity (Figure 6). A substantial agreement ( $\kappa = 0.80$ ,  $p < 0.001$ ) is recorded with the DCE curve, as 90% of cases show agreement (Figure 7). Moreover, 10% of cases have a disagreement with quite high sensitivity and specificity 90%, while FNR and FPR are 10% with FOR is 18%. MRS showed a poor agreement with the histopathological analysis as it showed disagreement in 60% of cases with quite low sensitivity and specificity 40%, 57% PPV with 75% for 43% FDR, 60% FNR and 40% overall accuracy (Figure 8).

The cutoff value of the choline position for malignant characterization is 3.15 ppm with 80% sensitivity and 15% specificity (Figure 9), as summarized in Table 6. The combined Mp-MRI data (all parameters) show a moderate agreement ( $\kappa = 0.435$ ) in which 21.7% of cases possess disagreement with 23.5% FDR and overall accuracy of 78%.

**Table 6.** Diagnostic performance of Choline Curve Parameters for Breast cancer Prediction, analyzed as the area under the curve

	Choline Value (mmol/l)	Choline Position
AUC*	0.931 (<0.001)	0.283 (<0.001)
CI**	0.833 – 0.916	0.104 – 0.396
SE***	0.064	0.091
Cutoff	0.35	3.15
Sensitivity	100%	80%
Specificity	25%	15%
PPV	57%	48.5%
NPV	93%	55.5%

\*AUC = Area under the Curve, \*\*CI = Confidence Interval, \*\*\*SE = Standard Error, \*Null hypothesis: true area = 0.5

On the other hand, combined Mp-MRI data after omitting MRS data show almost perfect agreement ( $\kappa = 0.923$ ) with histopathological data and recorded 100% specificity, 90% sensitivity, 5% FDR and zero% for both FOR and FNR.

### Interrater reliability

Regarding the inter-rater reliability, consensus agreement, according to Cohen's kappa coefficient ( $\kappa$ ), was rated with an almost perfect agreement in the interpretation of DCE-MRI curves, MR-DWI, and MRS with  $\kappa = 0.92, 0.90$  and  $0.84$  respectively while morphological analysis showed a substantial agreement with  $\kappa=0.79$ .

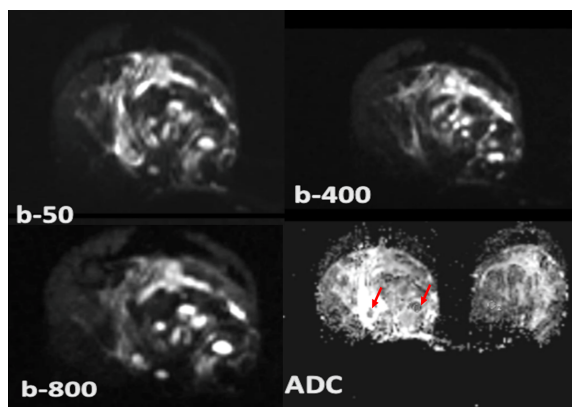


**Figure 4.** Idiopathic granulomatous mastitis. DWI show restricted diffusion on high b value with a low value on the ADC map (arrowed).

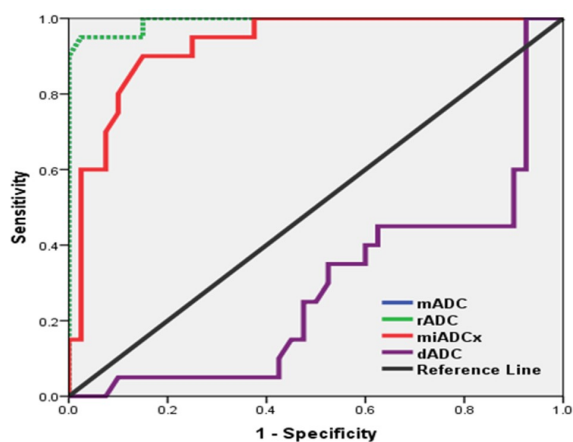


**Figure 5.** ROC curve for breast cancer prediction by ADC quantification

### DISCUSSION

Breast MRI is an essential portion of breast imaging that is recognized by the European and American guidelines as an accurate diagnostic tool (Kuhl, 2007; Ebrahim et al., 2018). Researchers employed the combination of MRI parameters to improve breast MRI diagnostic accuracy. Combining the morphological and functional MR data aims to provide data about cellularity, vascularity, neoangiogenesis, and metabolic activity (Pinker et al., 2017).

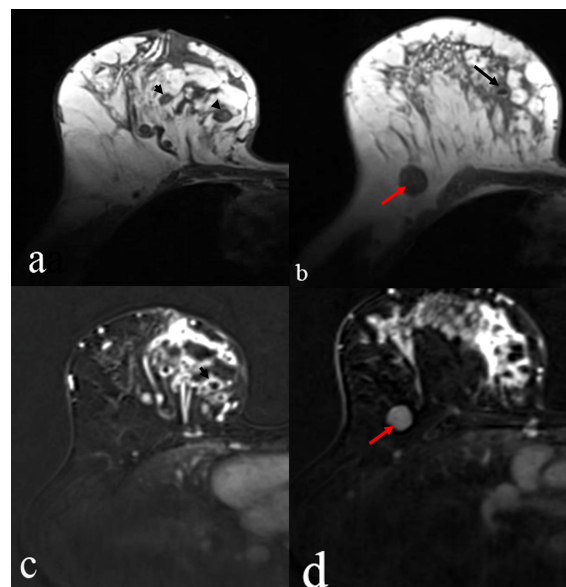


**Figure 6.** A 46-year female patient presented with idiopathic granulomatous mastitis. Axial pre-contrast T1-weighted image (a,b) and T2-weighted image (c,d) with fat saturation showed regional increase signal intensity of fibro-glandular parenchyma with small cystic areas (head arrows) and one show air-fluid level (long black arrow). Enlarged right axillary lymph (red arrow).

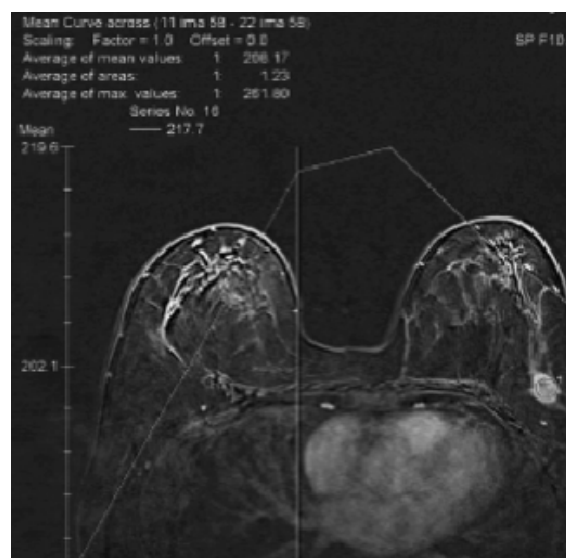


**Figure 7.** Washout (type 3) kinetic curve from DCE-MRI of upper-outer quadrant left breast, which was strongly enhanced mass during the arterial phase and then began to wash out.

In the current study, according to an agreement between different MRI parameters and histopathological analysis and validity measures of the different MRI parameters, spectroscopy results were identified as a weak predictor for breast cancer.

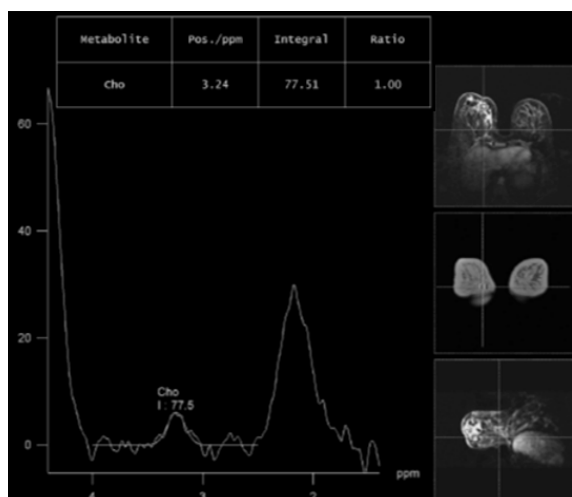


**Figure 8.** Right breast invasive ductal carcinoma. Single-voxel <sup>1</sup>H-MRS positioning and spectrum acquired from the voxel, indicating the resonances of total Choline-containing metabolites (tCho) at 3.24ppm.

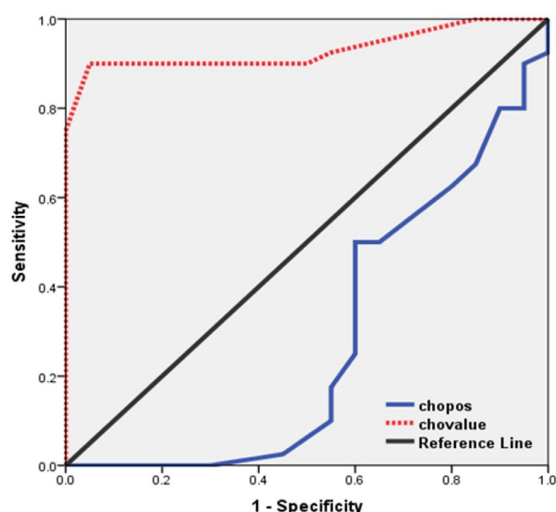


**Figure 9.** ROC curve for breast cancer prediction by total Choline position in ppm within the metabolite map.

When comparing the validity results for the combined Mp-MRI, including spectroscopy and excluding it, i.e., removing spectroscopy results, significant improvement in all validity measures was noted. According to these improvements, we oppose the conclusion of Aribal et al. (2016) that combined Mp-MRI does not improve and may reduce the diagnostic accuracy. Instead, we suggest tailoring combined multiparametric data, including morphology, diffusion, and dynamic enhancement curve, while Aribal et al. confined their assessment to functional imaging only (Aribal et al., 2016). Our result was in line with Zhang et al. who concluded that Mp-MRI, including both DCE-MRI and DWI, have a high diagnostic accuracy (AUC=0.971) (Zhang et al.,

2019). Rahbar and Partridge (Rahbar and Partridge, 2016) consider DCE-MRI cornerstone in the multiparametric assessment. In the current study, DCE is showing high sensitivity of 90%. A higher sensitivity of 97.3% reported by Aribal et al. (2016) and a sound sensitivity 100% recorded by Ebrahim et al. (2018). These studies show specificity 88.9% and 76%, respectively, compared to 90% in the present research. This specificity increased by 10% on using tailored combined data with a 5% false discovery rate. Hence, we agree with Pinker et al., 2017 that combined MRI parameters have been investigated to overcome DCE specificity issues.

MRI-DWI shows restricted diffusion in the majority of fatal cases in the current study; this is in agreement with Greenwood et al. (2018) that the malignant neoplasms have increased cellularity, leading to reduced and restricted diffusion of water molecules. Even that -in the current study- mean and relative ADC revealed the best performance among quantitative assessment of diffusion according to AUC, approving Yilmaz et al. (2018) conclusion that m-ADC and r-ADC are useful for the differentiation of benign from malignant breast masses. Moreover, opposing Hirano et al. (2012) on glorifying the role of d-ADC value as it has the least diagnostic performance in our results. Also, the current study agreed with Surov et al. (2019) meta-analyses that showed an m-ADC threshold value of  $1.0 \times 10^{-3} \text{ mm}^2 / \text{sec}$  could be used clinically as a limit for the differentiation of malignant and benign breast lesions, regardless of the Tesla strength, b values, and measurement methods.

The morphological analysis shows a high overall sensitivity of 97.5% and 85% specificity. These results are in agreement with Ebrahim et al. (2018) when concluding that the shape and margin of the lesions have a significant association with histopathological correlation. The spiculated margin of malignant lesions is the cornerstone in considering malignant nature in the morphological characterization, with an overall accuracy of 93.3% in the present study. That is quite similar to Moy et al. (2009) and slightly lower than Akita et al. with accuracy 96%. (Akita et al., 2009).

The current study results agree with Bolan (2013) who stated that spectroscopic analysis is unlike the brain and prostate, only depending on a single voxel as the elevation of choline metabolite in malignant lesions. Still, MRS established the least diagnostic efficiency in the current study results. Among this study limitations; is the retrospective nature of this study and the unavailability of MR-guided biopsy in our locality. Among the strengths points of the current study was excellent interrater reliability regarding the DCE-MRI and DWI and using four different quantitative ADC parameters to assess the diagnostic efficacy of DWI.

## CONCLUSION

Tailored Mp-MRI, including combined morphological, DWI, and dynamic enhancement curves, is an accurate non-invasive diagnostic procedure for the diagnosis of indeterminate breast lesions; this accuracy could help in the reduction of frequency of the unmerited biopsy procedure. The most useful quantitative biomarker parameters of ADC are mean and relative ADC values.

## List of abbreviations

ACR	American college of radiology
ADC	Apparent Diffusion coefficient
BI-RADS	Breast imaging reporting and data system
d-ADC	Difference ADC
DCE	Dynamic contrast enhancement
DWI	Diffusion-weighted imaging
FDR	False discovery rate
FNR	False-negative rate
FOR	False omission rate
FPR	False-positive rate
m-ADC	Mean ADC
Min-ADC	Minimum ADC
Mp-MRI	Multiparameteric MRI
MRS	MR spectroscopy
NPV	Negative predictive value
PPV	Positive predictive value
r-ADC	Relative ADC
ROC	Receiver operation characteristics
ROI	Region of interest
t-CHO	Total choline

## Research Ethics

This study was performed in accordance with the Declaration of Helsinki and received approval by the local ethical board of South Egypt cancer institute is having code SECI-IRB IORG0006563 approval number 424.

## Conflict of interest

Authors declare that they have no conflicts of interest. No external funding was employed in the current study.

## References

- Akita, A., Tanimoto, A., Jinno, H., Kameyama, K., and Kuribayashi, S. (2009). The clinical value of bilateral breast MR imaging: Is it worth performing on patients showing suspicious microcalcifications on mammography? *Eur. Radiol.* *19*, 2089–2096.
- Aribal, E., Asadov, R., Ramazan, A., Ugurlu, M.Ü., and Kaya, H. (2016). Multiparametric breast MRI with 3T: Effectivity of combination of contrast enhanced MRI, DWI and 1H single voxel spectroscopy in differentiation of Breast tumors. *Eur. J. Radiol.* *85*, 979–986.
- Baek, H.-M. (2012). Diagnostic Value of Breast Proton Magnetic Resonance Spectroscopy at 1.5T in Different Histopathological Types. *Sci. World J.* *2012*, 1–8.
- Bartella, L., and Huang, W. (2007). Proton ( 1 H) MR Spectroscopy of the Breast. *RadioGraphics* *27*, S241–S252.
- Bluemke, D.A., Gatsonis, C.A., Chen, M.H., DeAngelis, G.A., DeBruhl, N., Harms, S., Heywang-Köbrunner, S.H., Hylton, N., Kuhl, C.K., Lehman, C., et al. (2004). Magnetic Resonance Imaging of the Breast Prior to Biopsy. *JAMA* *292*, 2735–2742.
- Bolan, P.J. (2013). Magnetic Resonance Spectroscopy of the Breast: Current Status. *Magn. Reson. Imaging Clin. N. Am.* *21*, 625–639.
- Cilotti, A., Iacconi, C., Marini, C., Moretti, M., Mazzotta, D., Traino, C., Naccarato, A.G., Piagneri, V., Giacconi, C., Bevilacqua, G., et al. (2007). Contrast-enhanced MR imaging in patients with BI-RADS 3-5 microcalcifications. *Radiol. Med.* *112*, 272–286.
- Ebrahim, Y.G.S., Louis, M.R., and Ali, E.A. (2018). Multi-parametric dynamic contrast enhanced MRI, diffusion-weighted MRI and proton-MRS in differentiation of benign and malignant breast lesions: Imaging interpretation and radiology-pathology correlation. *Egypt. J. Radiol. Nucl. Med.* *49*, 1175–1181.
- Fowler, A.M. (2014). A molecular approach to breast imaging. *J. Nucl. Med.* *55*, 177–180.
- Gökalp, G., and Topal, U. (2006). MR imaging in probably benign lesions (BI-RADS category 3) of the breast. *Eur. J. Radiol.* *57*, 436–444.
- Greenwood, H.I., Freimanis, R.I., Carpentier, B.M., and Joe, B.N. (2018). Clinical Breast Magnetic Resonance Imaging: Technique, Indications,

- and Future Applications. In *Seminars in Ultrasound, CT and MRI*, (Elsevier), pp. 45–59.
- Haddadin, I.S., McIntosh, A., Meisamy, S., Corum, C., Snyder, A.L.S., Powell, N.J., Nelson, M.T., Yee, D., Garwood, M., and Bolan, P.J. (2009). Metabolite quantification and high-field MRS in breast cancer. *NMR Biomed.* 22, 65–76.
- Hirano, M., Satake, H., Ishigaki, S., Ikeda, M., Kawai, H., and Naganawa, S. (2012). Diffusion-weighted imaging of breast masses: Comparison of diagnostic performance using various apparent diffusion coefficient parameters. *Am. J. Roentgenol.* 198, 717–722.
- El Khoury, M., Lalonde, L., David, J., Labelle, M., Mesurrolle, B., and Trop, I. (2015). Breast imaging reporting and data system (BI-RADS) lexicon for breast MRI: Interobserver variability in the description and assignment of BI-RADS category. *Eur. J. Radiol.* 84, 71–76.
- Kuhl, C.K. (2007). Current status of breast MR imaging: Part 2. Clinical applications. *Radiology* 244, 672–691.
- Kuhl, C.K., Mielcareck, P., Klaschik, S., Leutner, C., Wardelmann, E., Gieseke, J., and Schild, H.H. (1999). Dynamic Breast MR Imaging: Are Signal Intensity Time Course Data Useful for Differential Diagnosis of Enhancing Lesions? *Radiology* 211, 101–110.
- Leonard, A.R., and Arnold, M.F. (1961). An Epidemiologic Approach to Health Education. *Am. J. Public Heal. Nations Heal.* 51, 1555–1560.
- Mango, V.L., Morris, E.A., David Dershaw, D., Abramson, A., Fry, C., Moskowitz, C.S., Hughes, M., Kaplan, J., and Jochelson, M.S. (2015). Abbreviated protocol for breast MRI: Are multiple sequences needed for cancer detection? *Eur. J. Radiol.* 84, 65–70.
- McPherson, K. (2000). ABC of breast diseases: Breast cancer---epidemiology, risk factors, and genetics. *BMJ* 321, 624–628.
- Moy, L., Elias, K., Patel, V., Lee, J., Babb, J.S., Toth, H.K., and Mercado, C.L. (2009). Is Breast MRI Helpful in the Evaluation of Inconclusive Mammographic Findings? *Am. J. Roentgenol.* 193, 986–993.
- Park, M.J., Cha, E.S., Kang, B.J., Ihn, Y.K., and Baik, J.H. (2007). The Role of Diffusion-Weighted Imaging and the Apparent Diffusion Coefficient (ADC) Values for Breast Tumors. *Korean J. Radiol.* 8, 390.
- Pinker, K., Bogner, W., Gruber, S., Brader, P., Trattig, S., Karanikas, G., and Helbich, T.H. (2011). Molecular Imaging in Breast Cancer – Potential Future Aspects. *Breast Care* 6, 110–119.
- Pinker, K., Helbich, T.H., and Morris, E.A. (2017). The potential of multiparametric MRI of the breast. *Br. J. Radiol.* 90, 20160715.
- Rahbar, H., and Partridge, S.C. (2016). Multiparametric MR Imaging of Breast Cancer. *Magn. Reson. Imaging Clin. N. Am.* 24, 223–238.
- Rao, A.A., Feneis, J., Lalonde, C., and Ojeda-Fournier, H. (2016). A Pictorial Review of Changes in the BI-RADS Fifth Edition. *RadioGraphics* 36, 623–639.
- Razek, A.A.K.A., Gaballa, G., Denewer, A., and Nada, N. (2010). Invasive ductal carcinoma: correlation of apparent diffusion coefficient value with pathological prognostic factors. *NMR Biomed.* 23, 619–623.
- Schnall, M.D., Blume, J., Bluemke, D.A., DeAngelis, G.A., DeBruhl, N., Harms, S., Heywang-Köbrunner, S.H., Hylton, N., Kuhl, C.K., Pisano, E.D., et al. (2006). Diagnostic Architectural and Dynamic Features at Breast MR Imaging: Multicenter Study. *Radiology* 238, 42–53.
- Shimauchi, A., Ota, H., Machida, Y., Yoshida, T., Satani, N., Mori, N., Takase, K., and Tozaki, M. (2016). Morphology evaluation of nonmass enhancement on breast MRI: Effect of a three-step interpretation model for readers' performances and biopsy recommendations. *Eur. J. Radiol.*
- Shimauchi, A., Machida, Y., Maeda, I., Fukuma, E., Hoshi, K., and Tozaki, M. (2018). Breast MRI as a Problem-solving Study in the Evaluation of BI-RADS Categories 3 and 4 Microcalcifications: Is it Worth Performing? *Acad. Radiol.* 25, 288–296.
- Spak, D.A., Plaxco, J.S., Santiago, L., Dryden, M.J., and Dogan, B.E. (2017). BI-RADS® fifth edition: A summary of changes. *Diagn. Interv. Imaging* 98, 179–190.
- Stusińska, M., Szabo-Moskal, J., and Bobek-Billewicz, B. (2014). Diagnostic value of dynamic and morphologic breast MRI analysis in the diagnosis of breast cancer. *Polish J. Radiol.* 79, 99–107.
- Surov, A., Meyer, H.J., and Wienke, A. (2019). Can apparent diffusion coefficient (ADC) distinguish breast cancer from benign breast findings? A meta-analysis based on 13 847 lesions. *BMC Cancer* 19, 955.
- Uematsu, T., Yuen, S., Kasami, M., and Uchida, Y. (2007). Dynamic contrast-enhanced MR imaging in screening detected microcalcification lesions of the breast: is there any value? *Breast Cancer Res. Treat.* 103, 269–281.
- Yilmaz, E., Sari, O., Yilmaz, A., Ucar, N., Aslan, A., Inan, I., and Parlakkılıç, U.T. (2018). Diffusion-

Weighted Imaging for the Discrimination of Benign and Malignant Breast Masses; Utility of ADC and Relative ADC. *J. Belgian Soc. Radiol.* 102.

Zhang, M., Horvat, J. V, Bernard-Davila, B., Marino, M.A., Leithner, D., Ochoa-Albiztegui, R.E., Helbich, T.H., Morris, E.A., Thakur, S., and

Pinker, K. (2019). Multiparametric MRI model with dynamic contrast-enhanced and diffusion-weighted imaging enables breast cancer diagnosis with high accuracy. *J. Magn. Reson. Imaging* 49, 864–874.

### **Egyptian Association for Cancer Research (EACR)**

<http://eacr.tanta.edu.eg/>

EACR is an NGO society that was declared by the Ministry of Social Solidarity (Egypt) No. 1938 in 19/11/2014 based on the initiative of Prof. Mohamed Labib Salem, the current Chairman of EACR. EACR aims primarily to assist researchers, in particular young researchers in the field of cancer research through workshops, seminars and conferences. Its first international annual conference entitled "Anti-Cancer Drug Discovery" was successfully organized in April 2019 (<http://acdd.tanta.edu.eg>). Additionally, EACR aims to raise the awareness of the society about the importance of scientific research in the field of cancer research in prediction, early diagnosis and treatment of cancer. EACR is also keen to outreach the scientific community with periodicals and news on cancer research including peer-reviewed scientific journals for the publication of cutting-edge research. The official scientific journal of EACR is "International Journal of Cancer and biomedical Research (IJCBR: <https://jcbjournals.ekb.eg>) was successfully issued in 2017 and has been sponsored by the Egyptian Knowledge Bank (EKB: [www.ekb.eg](http://www.ekb.eg)).

**EACR Chairman,**

**Prof. Mohamed Labib Salem, PhD**

Professor of Immunology

Faculty of Science, Tanta University, Egypt

**International Journal of Cancer & Biomedical Research**  
**(IJCBR) Online ISSN 2682-2628**

**Editor-in-Chief**

---

**Mohamed Labib Salem, PhD**  
Tanta University, Egypt

**Managing Editor**

---

**Nehal Elmashad, MD**  
Tanta University, Egypt

**Nabil Mohy Eldin, PhD**  
Kafrelsheikh University, Egypt

**Doaa Al-Ghareeb, PhD**  
Alexandria University, Egypt

**Abdel-Aziz Zidan, PhD**  
Damanhour University, Egypt

**Wesam Meshrif, PhD**  
Tanta University, Egypt

**Rasha Eraky, MD**  
Tanta University, Egypt

**Associate Editor**

---

**Hesham Tawfik**  
Tanta University, Egypt

**Mostafa El-Sheekh**  
Tanta University, Egypt

**Yousry Albolkin, PhD**  
Tanta University, Egypt

**Gamal Badr**  
Assuit University, Egypt

**Elsayed Salim**  
Tanta University, Egypt

**Essam Elshiekh**  
Tanta Cancer Center, Egypt

**Editorial Board**

---

**Alberto Montero**  
Taussig Cancer Center,  
Cleveland, USA

**Marcela Diaz**  
Cleveland Clinic Foundation, USA

**Yi Zhang**  
Zhengzhou University, China

**Shengdian Wang**  
Chinese Academy of Sciences,  
China

**Faris Alenzi**  
Prince Sattam bin Abdulaziz  
University, KSA

**Mark Robunstein**  
Medical University of South  
Carolina, USA

**Mamdooh Ghoneum, DSC**  
Charles Drew University of  
Medicine & Science, USA

**Natarajan Muthusamy, DVM**  
The Ohio State University, USA

**Hideki Kasuya MD, PhD,**  
**FACS**  
Nagoya University, Japan

**Sherif El-Khamisy, MD**  
Sheffield University, UK

**Mohamed Abou-El-Enein,**  
**MD**  
Charité Universitätsmedizin  
Berlin, Germany

**Alaa Eldin Almostafa, MD**  
McGill University, Canada

**Amr Amin**  
United Arab Emirates  
University, UAE

**AbdelRahman Zekri**  
National Cancer Institute, Egypt

**Mohamed Attia, MD**  
Tanta University, Egypt

**Mohamed Elshanshory, MD**  
Tanta University, Egypt

**Hussein Khamis**  
Alexandria University, Egypt

**Magdy Mahfouz**  
Kafr Elsheikh University, Egypt

**Ehab Elbedewey**  
Tanta University, Egypt

**Abeer Badr**  
Cairo University, Egypt

**Nadia Hamdy, PharmD**  
Ain Shams University, Egypt

**Ibrahim El-Sayed**  
Menoufia University, Egypt

**Tarek Aboul-Fadl, PharmD**  
Assiut University, Egypt

**Mohamed Noureldin**  
Banaha University, Egypt

**Haiam Abou Elela**  
National Institute of  
Oceanography and Fisheries,  
Egypt

**Sameh Ali, MD**  
Nationa Liver Institute, Egypt

**Maha EL-Demellawi**  
City for Scientific Research &  
Technology Applications, Egypt

**Desouky A Abd-El-Haleem**  
City for Scientific Research &  
Technology Applications, Egypt

**Ashraf Tabll**  
National Research Center, Egypt

**Wael Lotfy, MD**  
Alexandria University, Egypt

**Olfat Gadallah, MD**  
Tanta University, Egypt

**Nahla Shoukry**  
Suez University, Egypt

**Medhat Eldenary**  
Tanta University, Egypt

**Nagla Sarhan, MD**  
Tanta University, Egypt

**Naglaa Fathy, MD**  
Zagazik University, Egypt

**Azza Hasan Mohamed**  
Menoufia University, Egypt

**Nanees Gamal Eldin**  
Tanta University, Egypt

**Mohamed Mansour, UK**

**Sabbah Hammoury**  
Alexandria Ayadi Almostaqbal  
Oncology Hospital, Egypt

**Nehal Aboufotouh**  
Zewail City for Science and  
Technology, Cairo, Egypt

**Amir Elkhani**  
Galaxo, San Francisco, USA

**Rabab Khairat**  
National Research Center,  
Giza, Egypt

**Ahmed Alzohairy**  
Zagazi University, Egypt

**Wgady Khalil**  
National Research Center, Egypt

**Sayed Bakry**  
Alazhar University, Egypt

**Mohamed Ghanem, MD**  
Kafr Elshikh University, Egypt

**Mohamed Salama, MD**  
Mansoura University, Egypt

**Mona Marie, MD**  
Alexandria University, Egypt

**For more information, contact**

---

**Hamdi Kandil**  
Tanta University, Egypt  
Email: ljcb100@gmail.com